AUT Journal of Mechanical Engineering

AUT J. Mech. Eng., 6(2) (2022) 279-292
DOI: 10.22060/ajme.2022.19980.5978

Numerical and Thermodynamic Study of a Gas Turbine Cycle with Evaporative Cooling

G. Ghassabi*, S. E. Shakib, M. Ebadian

Department of Mechanical Engineering, Bozorgmehr University of Qaenat, Qaen, Iran

ABSTRACT: It has been demonstrated that thermal efficiency can be improved and Nox emission can be reduced in gas turbine cycles by inlet air evaporative cooling. For this method, few studies have been performed using numerical simulations due to the complexity of the combustion and evaporation process. This study numerically and thermodynamically investigated the effect of inlet evaporative cooling on the thermal efficiency and NOx emission of a V94.2 gas turbine. The compressor and turbine are simulated using thermodynamic modeling. However, thermodynamic modeling could be able to calculate the temperature only at the inlet and outlet of devices. Analysis of evaporating cooling effect on combustion chamber temperature distributions and species distribution could be achieved by numerical method. Therefore, the combustion chamber was simulated by numerical modeling using Ansys Fluent 16. The process was simulated at four humidity ratios, including, 0, 25%, 50%, and 75%. Combustion was assumed to occur in a diffusion-type flame. The mass flow rate of fuel and air was 3.64 kg/s and 214.2 kg/s, respectively. Results show that Numerical and thermodynamic solutions have a good agreement with the empirical result. Also, it is observed that the accuracy of the numerical solution is better than the thermodynamic solution. Results indicated a 0.44% improvement in thermal efficiency and a considerable 33.5% reduction of NOx emission at the highest humidity ratio.

Review History:

Received: May, 01, 2021
Revised: Jan. 10, 2022
Accepted: Feb . 05, 2022
Available Online: Feb . 11, 2022

Keywords:

NOx
Turbulent flame
Thermal efficiency
Humidity ratio

1- Introduction

The rising demand for fossil fuels for various applications and their limited resources, as well as the steady pollutants emission into the environment, prompted several investigations into the fuel consumption performance of many pieces of equipment. Gas and steam power plants have a high rate of fuel consumption. Accordingly, several methods have been proposed to improve thermal efficiency and reduce consumption and pollutant emission in these plants.

Borat [1] investigated the effect of steam injection into a gas turbine, comparing a gas cycle and a combined cycle (gas and steam cycle) using a steam injection in terms of several parameters. The study relied on thermodynamic analysis, showing that the cycle becomes more efficient in both cases. However, the combined cycle was more effective in increasing the efficiency than the gas cycle with steam injection. In their numerical study of the effect of the gas turbine compartment geometry on the overall thermal efficiency, Sabunchi and Kheradmand [2] showed that removing the combustion chamber elbow does not significantly affect the thermal efficiency. Kim and Perez-Blanco [3] carried out a thermodynamic analysis, exploring the effects of water injection into the compressor inlet, as well as using a recuperator, on the increase in combustion chamber inlet temperature using the turbine exhaust. Their results showed that using the recuperator in tandem with water injection improves thermal efficiency and net output work by 6% and 270 kJ/kg, respectively. Sheikh Beigi and Ghofrani [4] thermodynamically investigated several gas turbine cycles equipped with a reheater and a recuperator heat exchanger. Results indicated that the heat exchanger improved the overall efficiency of the open cycle (heating)—especially at low turbine inlet temperatures (1000°C). In another thermodynamic study, De Pape et al. [5] used Aspen to simulate steam injection at the compressor outlet used in a micro gas turbine cycle equipped with a recuperator. The cycle was designed to allow heat transfer between the recuperator and both the compressor exhaust and the water. The study claimed that using the recuperator and injecting steam realize an 18% reduction in fuel consumption and a 7% increase in electrical efficiency. Deymi-Dashtebayaz et. al [6] improved the gas turbine efficiency using two inlet air cooling method. Through simulation, Zaki and Rajabi [7] examined the effects of the equivalence ratio on NOx generation in methane, propane, and pentane combustion. They demonstrated the significant role of the equivalence ratio in NOx generation for the three fuels. Comodi et al. [8] investigated the performance of a gas microturbine in warm climates by inlet air cooling with a Vapor-Compression Refrigeration System (VCRS). They concluded that the inlet VCRS-cooled raises the level of microturbine output under ISO conditions and boosts the power generation efficiency by

*Corresponding author's email: Ghodrat.ghassabi@buqaen.ac.ir

1.5%. Hassan Athari et al. [9] compared the exergy of a gas turbine with a combined cycle with steam injection and inlet air cooling in a thermodynamic analysis. The results showed that cooling and steam injection and the integration of the steam turbine with gas turbine cycles improve the efficiency of electrical systems. Adopting a thermodynamic approach, Murad Ali Pour Mohammad et al. [10] studied the effects of adding a recuperator to a microturbine, suggesting that using the recuperator can reduce fuel consumption by nearly 45%. EL-Shazly et al. [11] investigated the impacts of various inlet cooling techniques on the performance of an integrated gas turbine, comparing the thermal efficiency, power output, and fuel consumption of water-cooled (absorption refrigerator) and non-cooled gas turbines. Considerable thermal efficiency and power output improvements were reported for the cooled gas turbine. It should be noted that the present study compares the C++ simulation of a turbine with the results corresponding to an MS 6001 B turbine.

Taking a thermodynamic approach, Sahur and Sanjay [12] examined incorporating an intercooler into a cycle equipped with a recuperator, where the turbine blades were cooled by layered cooling. The results indicated that the specific work and the fuel consumption of the recuperator- and intercooler-equipped cycle are, respectively, 50% and 27.8% higher than the reference cycle. In another thermodynamic study [13], the authors examined the incorporation of an intercooler into a recuperator-equipped cycle that used layered cooling for turbine blades. Moreover, it was shown that the specific work and the fuel consumption of the recuperator- and intercooler-equipped cycle were, respectively, 50% and 27.8% higher than the reference cycle.

Amiri-Rad and Kazemian-Najafabadi [14] thermodynamically investigated a gas turbine cycle equipped with a recuperator and steam injection to specify the optimum steam temperature. They decided the optimum temperature was 318.5°C, at which the thermal efficiency increased by 4.6%. Relying on a genetic algorithm, Sanaye et al. [15] tried the multi-objective optimization approach for a power plant incorporating a gas turbine cycle with steam injection, a steam generator, and a cooling absorbent, reporting a thermal efficiency of 30.7% under optimum working conditions.

Pashchenko [16] carried out a thermodynamic analysis to evaluate the effects of incorporating a recuperator heated by the gas leaving the turbine. The recuperator was used for pre-heating of the steam and methane. Furthermore, the steam–methane mix was injected into the combustion chamber after preheating by the recuperator. The results show that the efficiency of the recuperator was undermined at elevated pressure.

Barakat et al. [17] proposed a novel hybrid cooling system, which included a heat exchanger with fogging, to improve the gas turbine efficiency. The results were suggestive of 50% less water consumption in the hybrid system than in the fogging system.

Ahmadzade and Rashidi [18] simulated the performance of gas turbine units with inlet air cooling. Their Result shows that the energy and exergy efficiencies increase using inlet air cooling.

According to the literature, inlet air evaporative cooling is a popular method to enhance gas turbine performance. Many thermodynamic and numerical studies have focused on evaporative cooling, but few numerical simulations adopt the Computational Fluid Dynamics (CFD) approach. Because the previous studies were focused on the enhancement of thermal efficiency without consideration of the pollutants emission. Therefore, the thermal efficiency of the gas turbine cycle was calculated thermodynamically using values of temperature on the boundary of devices, regardless of the temperature distribution of the combustion chamber. However, the temperature distribution of the combustion chamber is necessary for the prediction of NOx emission. More details of the combustion process, like fuel-air mixing rate, can be considered by CFD modeling. Moreover, given the complexity of the combustion process and the nonlinear nature of mass fraction equations for the species, only CFD modeling can estimate combustion chamber temperature distribution and species distribution precisely. The present study thermodynamically and numerically investigates the effect of evaporative cooling on NOx emission and thermal efficiency. The compressor and turbine are simulated using thermodynamic modeling. Thermodynamic modeling could be able to show the trend of the gas turbine cycle only at the inlet and outlet of devices. However, analysis of the evaporating cooling effect on temperature and species distributions could be achieved by the CFD method. Also, the location of hot spots is observable using CFD modeling. These advantages distinguish CFD modeling from thermodynamic modeling. Therefore, the combustion chamber is simulated using Ansys fluent 16 in the present study.

2- Introducing the Cycle with Inlet Evaporative Cooling

The schematic diagram of a gas power plant cycle with inlet evaporative cooling is shown in Fig. 1 (Cycle 1). As can be seen, first, water (line a) is added to ambient air (line b) in the air humidifier for air cooling. The humid air (line 1) enters the compressor. Then, the outlet compressor flow (line 2) enters the combustion chamber. Finally, the high temperature of the outlet combustion chamber (line 3) causes work output in the turbine.

In this research, the combustion chamber was modeled using Ansys Fluent 16, and the thermodynamic analysis of the power plant compressor and turbine was carried out by MATLAB code. Table 1 presents the required data and the input variables in both cycles. Four humidity ratios (0, 25%, 50%, and 75%) were considered for the cooling process.

3- Governing Equations and Numerical Simulation of the Combustion Chamber

Fig. 2 illustrates the gas turbine combustion chamber, which is equipped with a concentric double elbow and eight burners on top. Moreover, Fig. 3 depicts one of the burners. According to Fig. 2, the air is introduced from the outer elbow, which directs it to the upper section of the chamber, where it mixes with the methane coming from the burner. The fuel and air mix then combusts, and the products are transport

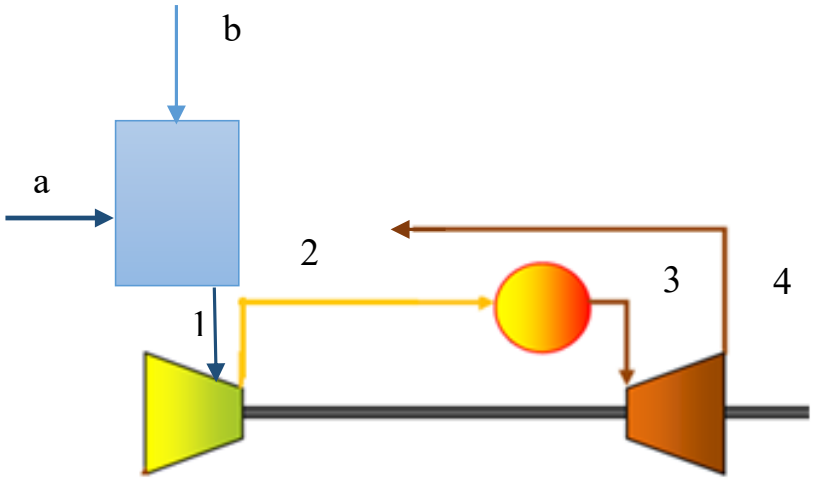

Fig. 1. Schematic diagram of a gas power plant cycle with inlet evaporating cooling

Table 1. Input variables for the regular cycle and Cycle 1

Input Variable	Value
Inlet Air intake T_a	295 K
Compressor Outlet Temperature T_2	623 K
Turbine Inlet Pressure (P_3)	830 kPa
Turbine Outlet Pressure (P_4)	100 kPa
Fuel Mass Flow Rate ($\dot{m}_f$)	3.64 $\frac{\text{kg}}{\text{s}}$
Air Mass Flow Rate ($\dot{m}_a$)	214.2 $\frac{\text{kg}}{\text{s}}$
The heating value of fuel (h_f)	50010 $\frac{\text{kJ}}{\text{kg}}$

from the center through the inner elbow tube. Fig. 4 shows the dimensions of the combustion chamber.

Methane combustion was assumed to occur in a diffusion-type flame. Further, the Simple algorithm was used to solve momentum equations, as well as for pressure discretization. A turbulent combustion flow was assumed, and the standard k-ε model was employed to represent the flow. This model is very popular and suitable for the simulation of industrial applications. The upwind differencing scheme was used to discretize the convective terms. The two transfer equations in this model—for calculating the kinetic energy (k) and the turbulence energy dissipation rate (ε)—can be solved as follows [19].

$$\frac{\partial}{\partial t}(\rho k)+\frac{\partial}{\partial x_i}(\rho k u_i)= \frac{\partial}{\partial x_i}(\alpha_k \mu_{eff}\frac{\partial k}{\partial x_j})+G_k+G_b-\rho\varepsilon-Y_m \quad (1)$$

$$\frac{\partial}{\partial t}(\rho\varepsilon)+\frac{\partial}{\partial x_i}(\rho\varepsilon u_i)=\frac{\partial}{\partial x_i}(\alpha_\varepsilon \mu_{eff}\frac{\partial \varepsilon}{\partial x_j})+ C_{1\varepsilon}\frac{\varepsilon}{K}(G_k+C_{3\varepsilon}G_b)-C_{2\varepsilon}\rho\frac{\varepsilon^2}{k} \quad (2)$$

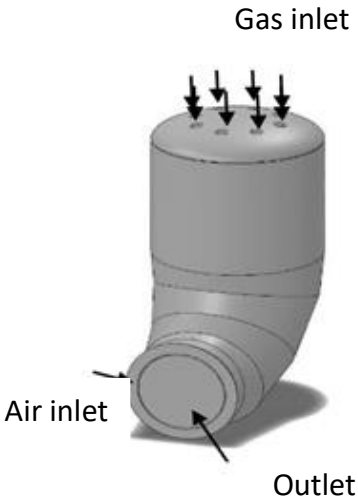

Fig. 4. Dimensions of the combustion chamber (mm)

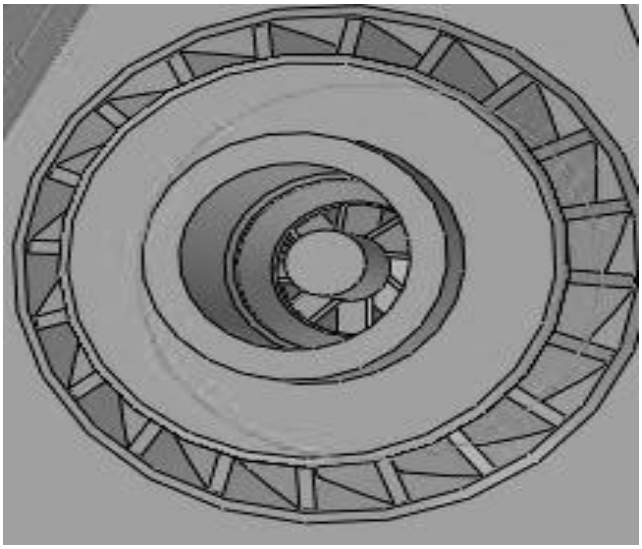

Fig. 3. A schematic of the burner

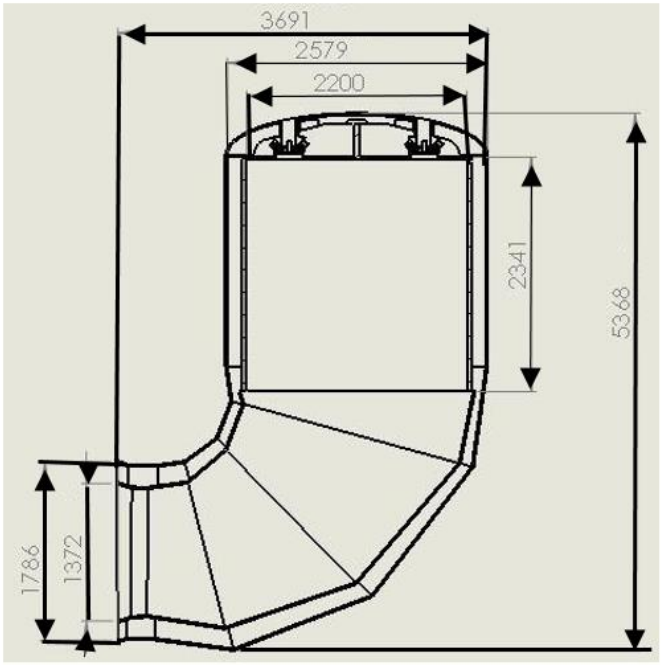

Fig. 4. Dimensions of the combustion chamber (mm)

Where G_k represents the turbulent energy generated by the change in the mean velocity, G_b denotes the turbulent energy generated by buoyancy, Y_m is the ratio of expansion perturbation in compressible turbulence to the overall turbulence energy dissipation rate. Previous studies [19] determined the equation constants at $C_\mu = 0.0845$, $\alpha_\varepsilon = 0.72$, $\alpha_k = 0.72$, $C_{2\varepsilon} = 1.68$, $C_{1\varepsilon} = 1.42$

The Magnussen model was employed for specifying the rate of combustion. This model is very simple and accurate for the simulation of Turbulent flame [20]:

$$R.R = A\rho \frac{\varepsilon}{k} \min(Y_f, \frac{Y_{O_2}}{S}) \tag{3}$$

Where $R.R$ is the reaction rate, A is an empirical constant (A = 4), Y is the fuel–oxygen mass fraction, S is the oxygen required by stoichiometry for the combustion of 1 kg fuel.

Further, the heat form developed by the Zeldovich mechanism [21] was used to model NOx, as follows:

$$\begin{aligned} O + N_2 &\xleftrightarrow{K_{\pm 1}} NO + N \\ N + O_2 &\xleftrightarrow{K_{\pm 2}} NO + O \\ N + OH &\xleftrightarrow{K_{\pm 3}} NO + H \end{aligned} \tag{4}$$

Where $K_{\pm 1,2,3}$ ($\frac{m^3}{mol.s}$) are the reciprocal reaction constants and are [22]:

$$\begin{aligned} K_1 &= 1.8\times10^8 \exp\left(-\frac{38370}{T}\right) \\ K_{-1} &= 3.8\times10^7 \exp\left(-\frac{425}{T}\right) \\ K_2 &= 1.8\times10^4 T \exp\left(-\frac{4680}{T}\right) \\ K_{-2} &= 3.81\times10^3 T \exp\left(-\frac{20820}{T}\right) \\ K_3 &= 7.1\times10^7 \exp\left(-\frac{450}{T}\right) \\ K_{-3} &= 1.7\times10^8 \exp\left(-\frac{24560}{T}\right) \end{aligned} \tag{5}$$

The rate of NO generation is obtained as follows [23]:

$$\begin{aligned} \frac{d[NO]}{dt} = {} & k_{+1}[O][N2] + k_{+2}[N][O2] + k_{+3}[N][OH] - \\ & k_{-1}[NO][N] - k_{-2}[NO][O] - k_{-3}[NO][H] \end{aligned} \tag{6}$$

As radiation between flame and walls is very effective on temperature distribution, Discrete Ordinates (DO) model was used for modeling the radiation [23]. Velocity inlet was the boundary condition for the air and fuel at the inlet, whereas pressure outlet was the boundary condition for the combustion products at the outlet. Moreover, the external wall was assumed to be insulated as the outer body of the combustion chamber was insulated.

Fig. 5 shows the average outlet temperature of the combustion chamber for a different number of grids. It is observed that the minimum number of hexagonal elements ensuring the grid independence of the results was determined at 47000. Furthermore, as the convergence criterion, residual levels were considered to remain below 10^{-5}. Fig. 6 depicts the combustion chamber and its computational meshwork made up of hexagonal elements.

4- Thermodynamic Model

In this study, the gas turbine cycle is a simple cycle that includes a compressor, a combustion chamber, and a gas turbine. In addition, the behavior of the compressor, gas turbine, and evaporative cooling was predicted using a code developed in MATLAB. In fact, this thermodynamic analysis was basically performed to determine the air temperature at the compressor and gas turbine outlets.

In contrast to the air standard Joule cycle, the irreversibility of practical turbomachines should be considered in the analysis of the gas turbine power plants using a simple cycle. Generally, the irreversibility of the turbomachines was determined by considering the associated isentropic efficiency

The following assumptions are normally considered in simulating the actual cycle of a gas turbine [24]:

- The cycle works in a steady state.
- In the ideal state, inlet air has the following volume fraction composition:

$$0.7748N_2 + 0.2059O_2 + 0.0003CO_2 + 0.019H_2O \tag{7}$$

- The ideal gas law was used for the air and combustion products.
- Compressor and turbine were considered adiabatic.
- Methane was the primary source of energy.

The humid air in the compressor was increased isentropically based on the following equation [24]:

$$\int C_{P-ha} \frac{dT}{T} = \frac{R}{\eta_P} \ln(\frac{P_2}{P_1}) \tag{8}$$

Where T is the temperature in Kelvin, P is the pressure in kPa, C_{P-ha} is the specific heat capacity of humid air in $\frac{kJ}{kg.K}$ and subscripts 1 and 2 denote the inlet and outlet conditions, respectively. Moreover, η_p is the polytropic efficiency of the compressor.

The thermodynamics properties of the air have a significant effect on the performance of the gas power cycle. It was supposed that the specific heat capacity of the stream passing from humid media is a function of the specific heat of the dry air and water as follows:

$$C_{P-ha} = C_{P-air} + \omega C_{P-water} \tag{9}$$

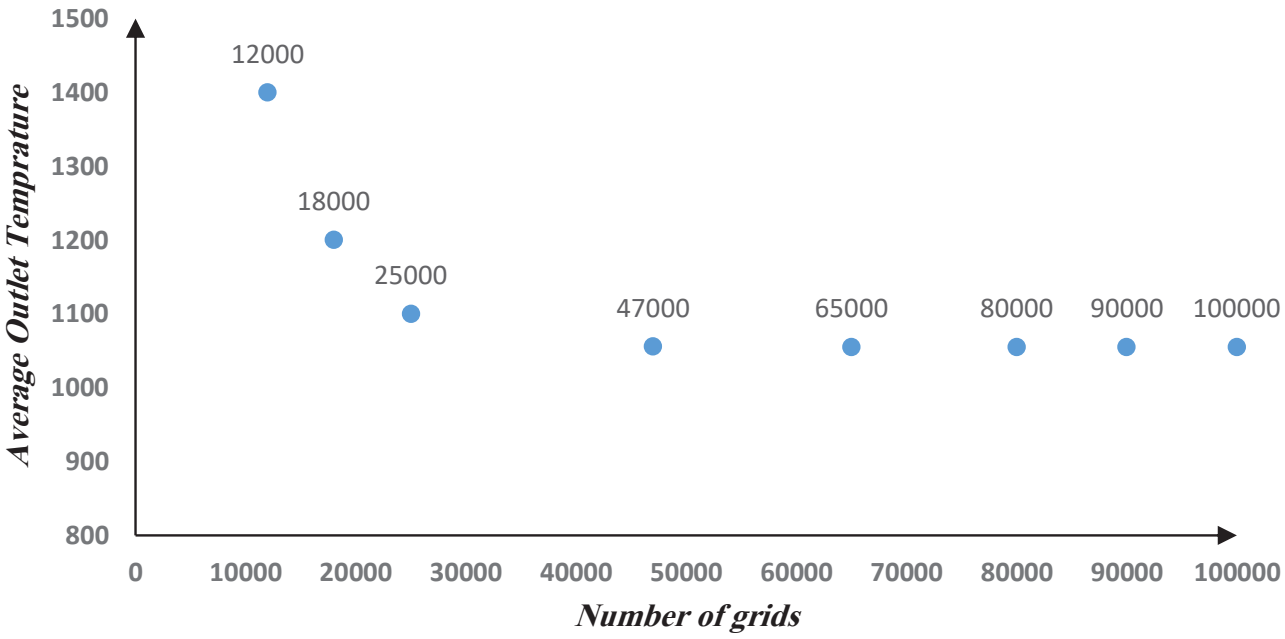

Fig. 5. The average outlet temperature of the combustion chamber for the different number of grids.

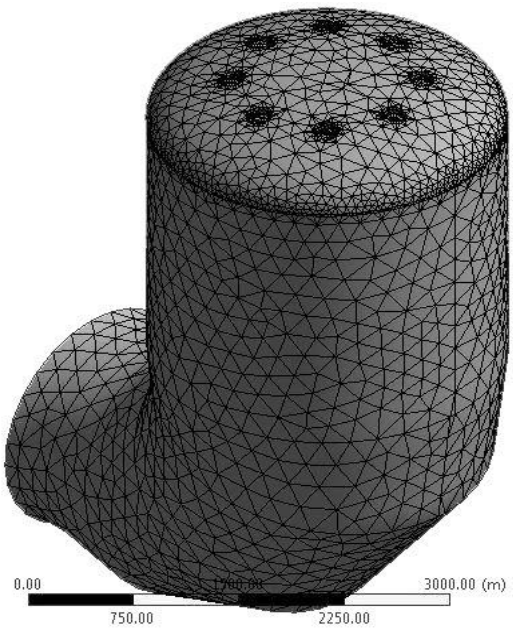

Fig. 6. The computational meshing of the combustion chamber

Table 2. Values of a, b, c, and d for different air elements and combustion products

Element	*a*	*B*	*c*	*d*
Nitrogen	30.418	2.544	0.238	0
oxygen	29.154	6.477	0.184	1.017
Carbon dioxide	51.128	4.368	1.469	0
Water	34.376	7.841	0.423	0

Table 3. Comparison between results.

Result	Average Outlet Temperature (K)	Error (%)	Average outlet NOx Mass fraction	Error (%)
Thermodynamic solution	1047	1.23	1.2E-7	4.35
Numerical solution	1056	0.38	1.17E-7	1.74
Empirical result [26]	1060	-	1.15E-7	-

Where ω is the absolute humidity of humid air entering the compressor. The specific heat capacity, enthalpy, and entropy values of every single element of air and combustion products were calculated using the following equation as a function of temperature [25].

$$C_P = a + by + cy^{-2} + dy^2 \tag{10}$$

$$h = 10^3[H^+ + ay + \frac{b}{2}y^2 - cy^{-1} + \frac{d}{3}y^3] \tag{11}$$

$$s = S^+ + a\ln(T) + by - \frac{c}{2}y^{-2} + \frac{d}{2}y^2 \tag{12}$$

$$y = T/1000 \tag{13}$$

It should be noted that the physical properties of air should be determined in terms of the volume fraction of its constituent elements. Therefore, on the condition that the humidity changes, the composition of the elements also will be varied, and consequently, the physical properties altered. Hence, the physical properties of the air in the simulator code were considered as a function of the humidity and air temperature in order to improve the accuracy of the calculations where *a, b, c*, and *d* are constants used for each of the air elements and combustion products, and *y* is a function of temperature. The values of these coefficients are given in Table 2 for nitrogen, oxygen, carbon dioxide, and water [25].

Similar to the previously mentioned equations for the compressor, the gas turbine outlet temperature was calculated using the following equation [24]:

$$\int C_P \frac{dT}{T} = R\eta_P \ln(\frac{P_2}{P_1}) \tag{14}$$

Where subscripts 3 and 4 refer to the turbine inlet and outlet, respectively. The flowchart of the solution of the thermodynamic developed model is shown in Fig. 7.

In Table 3, the average temperature at the combustion chamber outlet from the thermodynamic and the numerical solutions was compared with the data collected from Kaveh Qaen's power plant [26] to validate the accuracy of the results. Also, the average outlet NOx mass fraction from the thermodynamic and numerical solution was compared with the data collected from Kaveh Qaen's power plant [26] to validate the accuracy of the NOx results. The working conditions were similar to the regular cycle of the present study. The results revealed that the thermodynamic and the numerical solution errors were 1.23% and 0.38%, for temperature, respectively. Also, the thermodynamic and the numerical solution errors were 4.35 and 1.74% for NOx emission, respectively. Therefore, both results have a good agreement with empirical results. Moreover, the numerical result is in a better agreement with the empirical result than the thermodynamic solution, strongly suggesting the accuracy of the numerical solution.

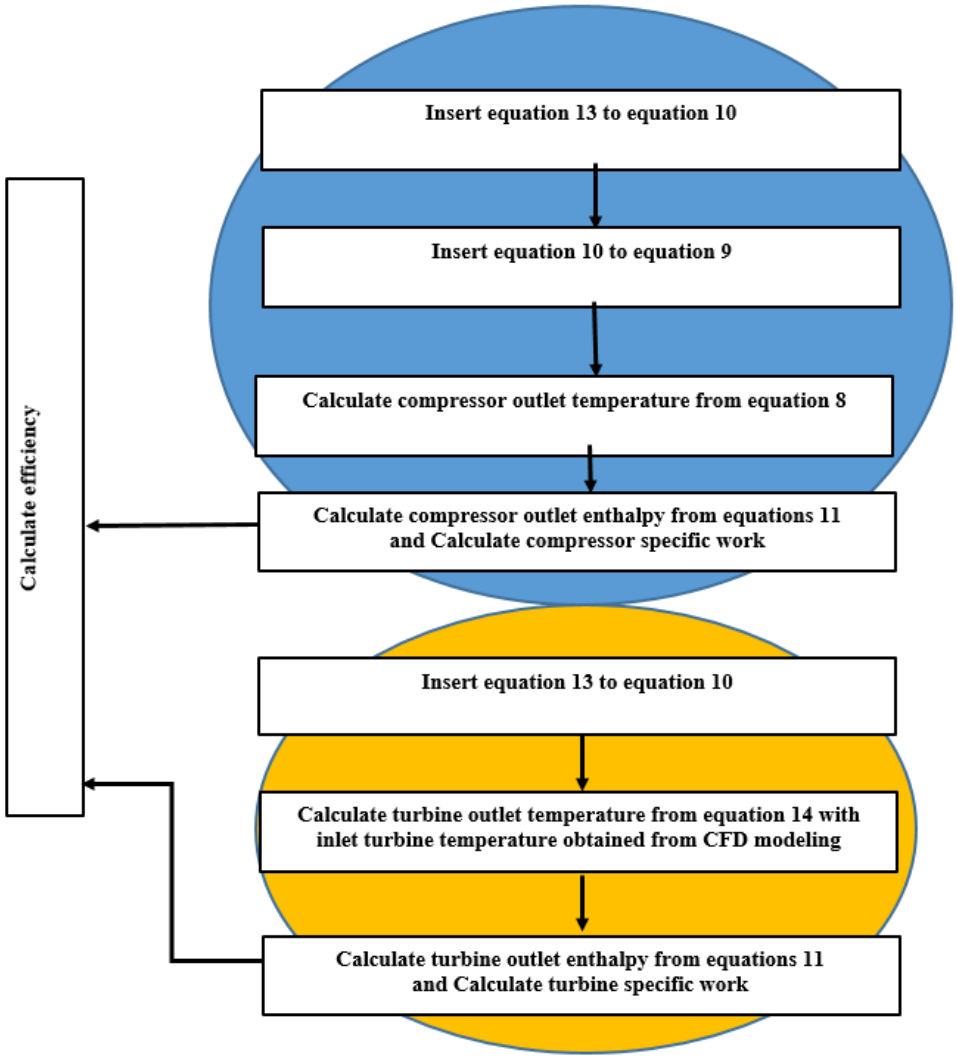

Fig. 7. Flowchart of the thermodynamic model solution

5- Results and Discussion

Fig. 8 shows the distribution of oxygen mass fraction. In both cases, the oxygen mass fraction remains fixed before the burner inlet but then decreases after mixing with the fuel and combustion. Moreover, the oxygen mass fraction increases by the secondary input air entering the holes placed around the combustion chamber. The oxygen mass fraction remained fixed before the outlet. A comparison of the two cases reveals that the rate of reaction and oxygen consumption reduces as a result of inlet air cooling. Accordingly, the mass fraction of oxygen in the outlet is higher in the case with inlet air cooling than that in a simple case.

In Fig. 9, the temperature distribution of the combustion chamber is shown in two cases with and without evaporative cooling. In both cases, the proximity of the burner, it is observed that the mixing of fuel and oxygen has caused combustion and a significant increase in temperature. In both cases, due to the contrast of radiation and the combustion chamber wall, and the secondary air dilution by cooling vents, the average flame temperature gradually decreases through the combustion chamber. By comparing the two cases, it is observed that in presence of evaporative cooling, flame temperature and flame length are reduced which has resulted in a significant reduction in the combustion chamber outlet temperature.

In Fig. 10, the mass fraction distribution of NOx is illustrated in two cases with and without evaporative cooling. It is observed that in both cases, in the flame zone and maximum temperature location, the mass fraction of NOx is maximized. Then a mass fraction of NOx decreases due to the decrease in temperature, the formation of other types, and dilution of combustion products using secondary air. Also by comparing two cases, it is observed that evaporative cooling caused a decrease in temperature and thus reducing the production of NOx.

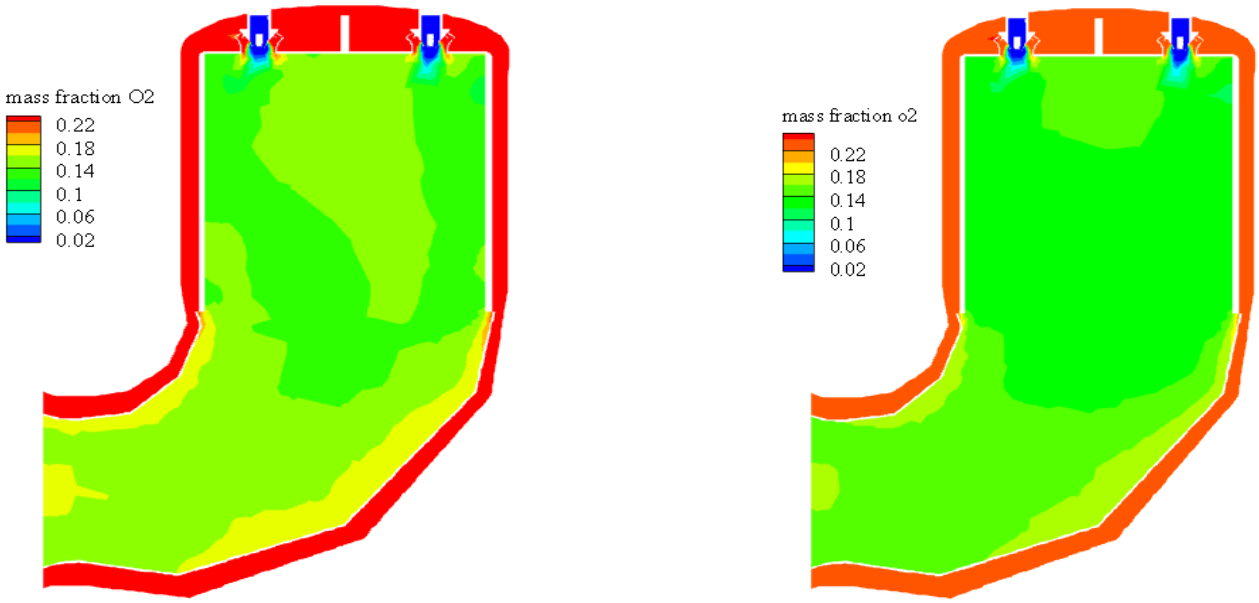

a) With evaporative cooling **b) Without evaporative cooling**

Fig. 8. The mass fraction distribution of oxygen with and without evaporative cooling

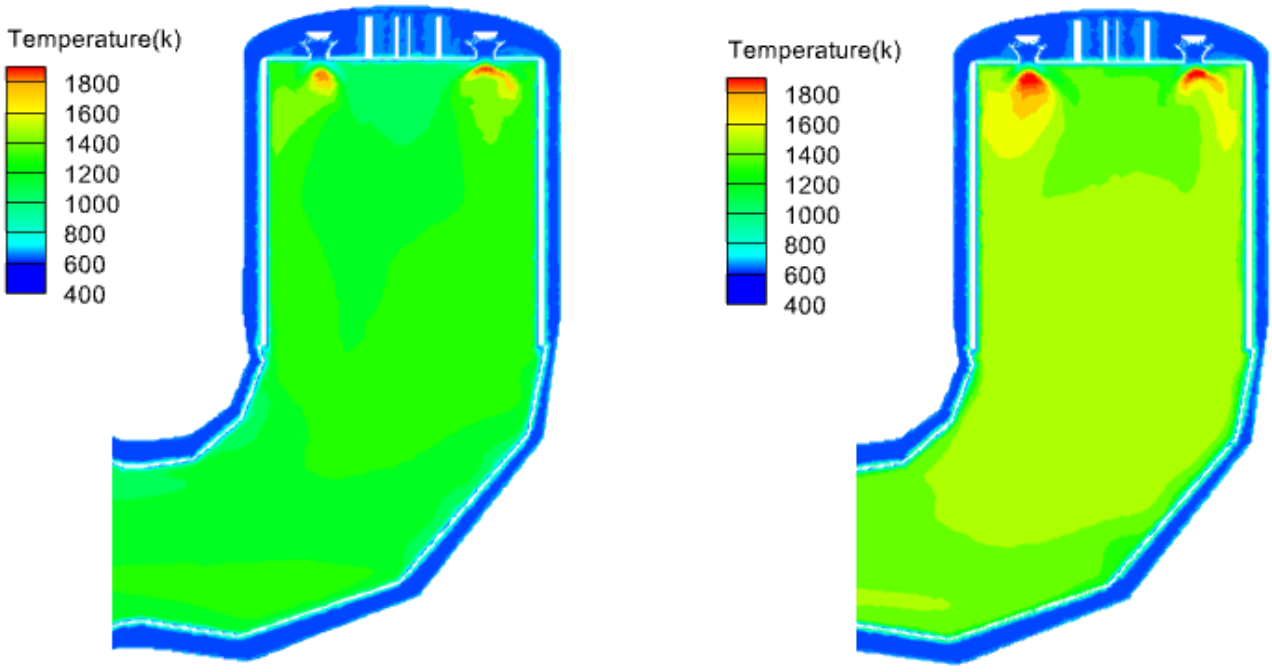

a) With evaporative cooling **b) Without evaporative cooling**

Fig. 9. Temperature distribution for two cases with and without evaporative cooling of entrance air

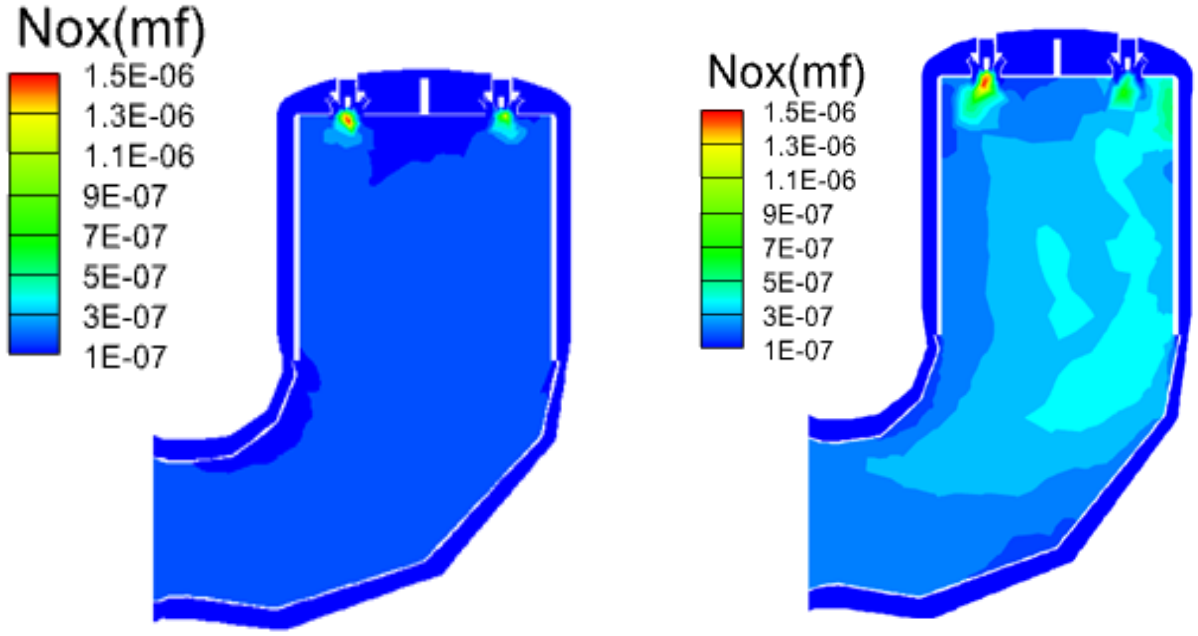

a) With evaporative cooling **b) Without evaporative cooling**

Fig. 10. The mass fraction distribution of NOx in two cases with and without evaporative cooling.

In Fig. 11, the effect of relative humidity of inlet air on the average outlet temperature of the combustion chamber is shown. It is observed that by increasing the relative humidity, the average outlet temperature decreases, and the amount of temperature reduction for the relative humidity of 75% is significant.

In Fig. 12, the relative humidity effect of inlet air on the thermal efficiency of the gas turbine is shown. It is observed that efficiency increases with increasing humidity due to increasing the mass flow rate and decreasing the inlet air temperature in the compressor. Moreover, according to the figure, in the maximum relative humidity, efficiency is increased by 0.44 % compared to the without an evaporative cooling case.

In Fig. 13, the relative humidity effect of inlet air on NOx emission is shown. It is observed that NOx emission decreases with increasing relative humidity due to the reduction in the combustion temperature. In addition, in maximum relative humidity, NOx emission is decreased by 33.5 % compared to the without an evaporative cooling case. Values of NOx reduction in the current study are in the same order as Ref. [27]. The water injection for NOx emission reductions of the gas turbine was investigated in [27]. Values of the inlet air relative humidity in the current study are in the same order as Ref. [27]. It is concluded that the portion of the water evaporated has the main role in NOx reduction in the water cooling method. Therefore, the evaporating cooling method is preferred over the water cooling method for reduction of water consumption. s

6- Conclusions

In this study, the effect of inlet air evaporative cooling on the thermal efficiency of a gas turbine and NOx emission were investigated in both numerical and thermodynamic method. The combustion chamber was simulated using Ansys Fluent 16 and the compressor and the turbine were analyzed thermodynamically using a Matlab code. Methane combustion was assumed to occur in a diffusion-type flame. The process was simulated at four humidity ratios, namely 0, 25, 50, and 75%. It was observed that in maximum relative humidity, efficiency increased by 0.44 % and NOx decreased by a considerable value of 33.5 %.

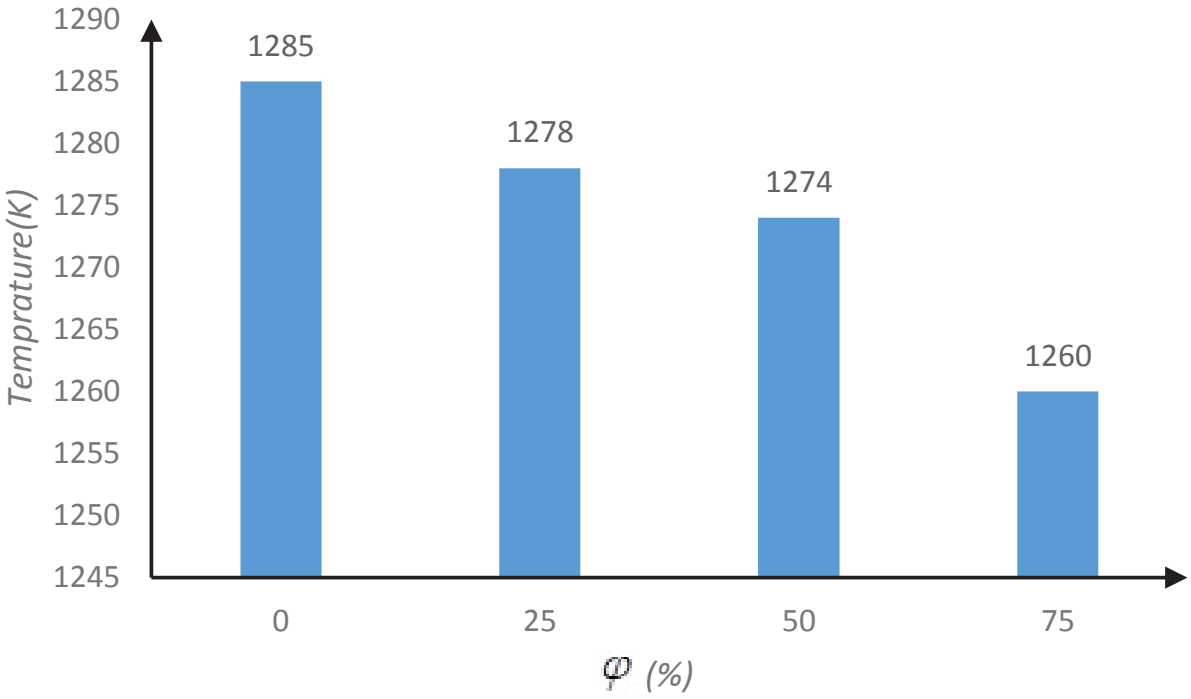

Fig. 11. Effect of relative humidity on average outlet temperature

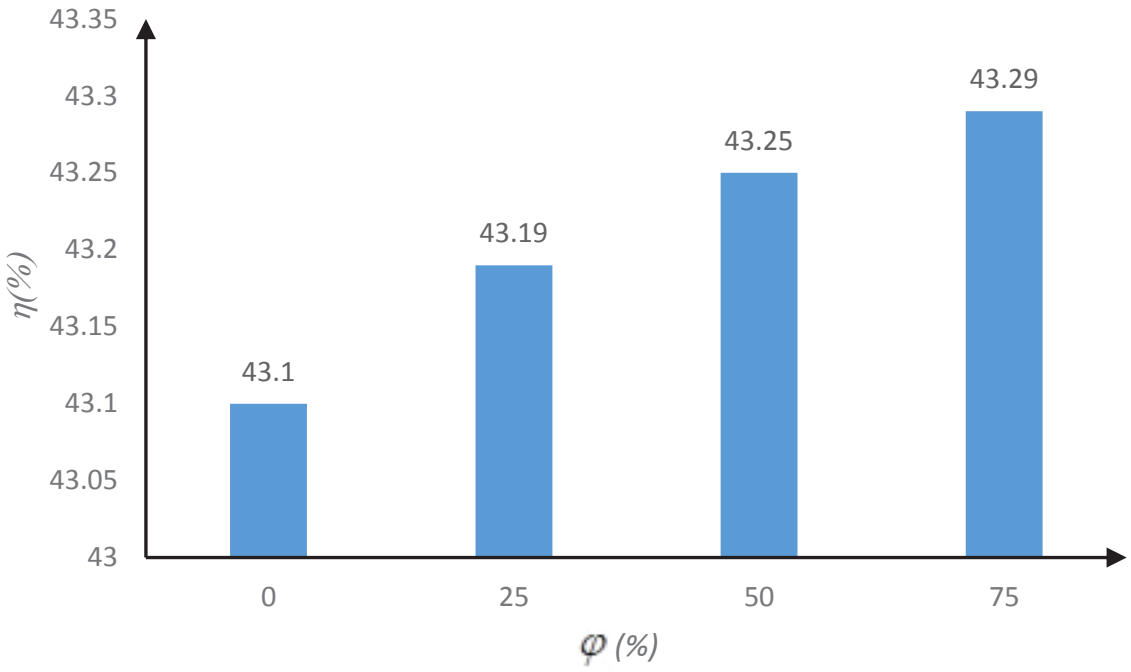

Fig. 12. The effect of relative humidity on thermal efficiency

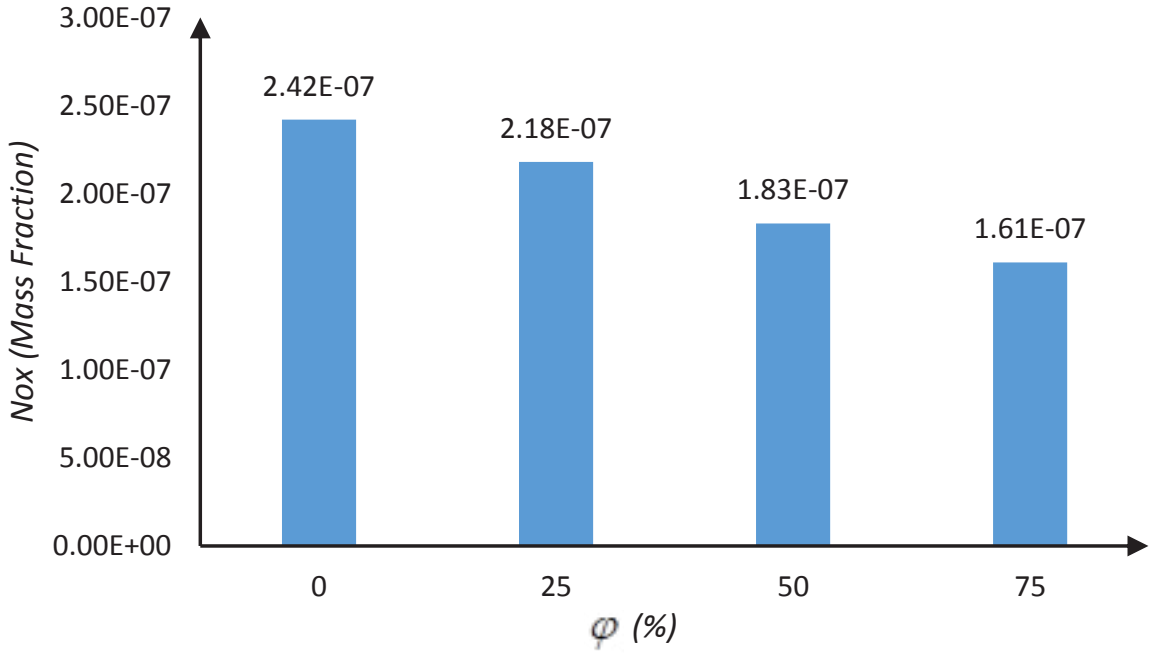

Fig. 13. The effect of relative humidity on NOx emission

References

[1] B. O, Efficiency improvement and superiority of steam injection in gas turbines, Energy Convers Manag 22 (1982) 13-18.

[2] K.S. A.Saboonchi, 3D-Numerical Gas Turbine Combustor, Esteghlal, 22 (2003) 137–148.

[3] P.-B.H. Kim KH, Potential of regenerative gas-turbine systems with high fogging compression, Appl Energy, 84 (2007) 16-28.

[4] G.M. Sheikhbeigi B, Thermodynamic and environmental consideration of advanced gas turbine cycles with reheat and recuperator, Int J Environ Sci Technol, 4 (2007) 253-262.

[5] D.F. De Paepe W, Bram S, De Ruyck J Steam injection experiments in a microturbine - A thermodynamic performance analysis, Appl Energy, 97 (2012) 569–576.

[6] D.-D.M. Farzaneh-Gord M, Arabkoohsar, Ahmad Khoshnevis AB, Akeififar H, Improving Khangiran gas turbine efficiency by two standard and one novel inlet air cooling method, Journal of the Brazilian Society of Mechanical Sciences and Engineering, 36 (2014) 571–582.

[7] M. Zaki, & Rajabi-Zargarabadi M, Numerical analysis of effects of primary aeration oN NOX production in a model gas turbine combustion chamber., Modares Mech Eng, 14 (2014) 101–108.

[8] R.M. Comodi G, Caresana F, Pelagalli L Enhancing micro gas turbine performance in hot climates through inlet air cooling vapour compression technique, Appl Energy, 147 (2015) 40-48.

[9] S.S. Athari H, Rosen MA, et al xergoeconomic study of gas turbine steam injection and combined power cycles using fog inlet cooling and biomass fuel, Renew Energy, 96 (2016) 715–726.

[10] M.A. Pourmohamad, Ashjari, M. A., & Khosroshahi ARR, Recuperator Energy and Exergy Analysis in the Application of Microturbine in Cogeneration of Heat and Power Systems, J Tabriz Univ Mech Eng, 46 (2016) 55-66.

[11] E.M. El-shazly AA, Sorour MM, El-maghlany WM, Gas turbine performance enhancement via utilizing different integrated turbine inlet cooling techniques, Alexandria Eng J, 55 (2016) 1903-1914.

[12] S. Mithilesh Kumar Sahur, Comparative Exergoeconomic Analysis of Basic and Reheat Gas Turbine with Air Film Blade Cooling., Energy, 132 160-170.

[13] S. Mithilesh Kumar, Thermoeconomic Investigation of Power Utilities: Intercooled Recuperated Gas Turbine Cycle Featuring Cooled Turbine Blades, Proceedings of the ICE - Energy, 138 (2017).

[14] K.-n.P. Amiri-rad E, Thermo-environmental and economic analyses of an integrated heat recovery steam-injected gas turbine, Energy, 141 (2017) 1940-1954.

[15] A.M. Sanaye S, Amani P, 4E modeling and multi-

criteria optimization of CCHPW gas turbine plant with inlet air cooling and steam injection, Sustain Energy Technol Assessments, 29 (2018) 70-81.

[16] P. D, Energy optimization analysis of a thermochemical exhaust gas recuperation system of a gas turbine unit., Energy Convers Manag, 171 (2018) 917–924.

[17] R.A. Barakat S, Hamed AM, Augmentation of gas turbine performance using integrated EAHE and Fogging Inlet Air Cooling System, Energy, 189 (2019) 116-133.

[18] M.A.H. Rashidi, Performance enhancement of gas turbine units by retrofitting with inlet air cooling technologies (IACTs): an hour - by - hour simulation study, Journal of the Brazilian Society of Mechanical Sciences and Engineering, 7 (2020).

[19] P. BS, Turbulence Flows, Cambridge University Press, 2007.

[20] F.F. Magnussen, Hjertager BH On mathematical models of turbulent combustion with special emphasis on soot formation and combustion, Symposium (International) on Combustion, 16 (1977) 719-729.

[21] J. Warnatz, Mass, U., & Dibble RW, Combustion, Springer, 2006.

[22] R.K. Hanson, & Salimian S Survey of Rate Constants in H/N/O Systems, Combustion Chemistry (1984) 420-361.

[23] [ANSYS in: Ansys Fluent 16 User's Guide, 2013.

[24] C.B. RES, FUNDAMENTALS OF THERMODYNAMICS, 7 ed., John Wiley & Sons, University of Michigan, 2009.

[25] A. Bejan, Tstsaroincs, G., & Moran M, Thermal design and optimization, Wiley, New York, 1996.

[26] Performance test of Kave combined cycle PP (GT V94.2), in.

[27] I.U. Block Novelo DA, Prakash V, Szymański A, Experimental investigation of gas turbine compressor water injection for NOx emission reductions, Energy, 176 (2019) 235–248.

HOW TO CITE THIS ARTICLE

G. Ghassabi, S. E. Shakib, M. Ebadian, Numerical and Thermodynamic Study of a Gas Turbine Cycle with Evaporative Cooling, AUT J. Mech Eng., 6 (2) (2022) 279-292.

DOI: 10.22060/ajme.2022.19980.5978